AAPS PharmSciTech, Vol. 14, No. 4, December 2013 (© 2013)
DOI: 10.1208/s12249-013-0021-7

Research Article

Evaluation of the Impacts of Formulation Variables and Excipients on the Drug Release Dynamics of a Polyamide 6,10-Based Monolithic Matrix Using Mathematical Tools

Oluwatoyin A. Adeleke,[1] Yahya E. Choonara,[1] Pradeep Kumar,[1] Lisa C. du Toit,[1] Lomas K. Tomar,[1] Charu Tyagi,[1] and Viness Pillay[1,2]

Received 10 May 2013; accepted 5 August 2013; published online 30 August 2013

Abstract. Drug release from hydrophilic matrices is regulated mainly by polymeric erosion, disentanglement, dissolution, swelling front movement, drug dissolution and diffusion through the polymeric matrix. These processes depend upon the interaction between the dissolution media, polymeric matrix and drug molecules, which can be significantly influenced by formulation variables and excipients. This study utilized mathematical parameters to evaluate the impacts of selected formulation variables and various excipients on the release performance of hydrophilic polyamide 6,10 (PA 6,10) monolithic matrix. Amitriptyline HCl and theophylline were employed as the high and low solubility model drugs, respectively. The incorporation of different excipient concentrations and changes in formulation components influenced the drug release dynamics as evidenced by computed mathematical quantities ($t_{x\%}$, $MDT_{x\%}$, f_1, f_2, k_1, k_2, and K_F). The effects of excipients on drug release from the PA 6,10 monolithic matrix was further elucidated using static lattice atomistic simulations wherein the component energy refinements corroborates the *in vitro* and *in silico* experimental data. Consequently, the feasibility of modulating release kinetics of drug molecules from the novel PA 6,10 monolithic matrix was well suggested.

KEY WORDS: excipients; formulation variables; mathematical tools; monolithic matrix; polyamide 6,10.

INTRODUCTION

The significance of hydrophilic polymer-based monolithic matrices as carriers for rate-modulated drug release has been on the increase as evidenced by the number of published manuscripts, patents and their applications in producing new commercially available drug products (1–3). To an extent, the prevalent and successful use of hydrophilic polymeric drug delivery systems can be associated with their ease of manufacturing, broad acceptance by the US Food and Drug Administration, relatively low cost of production, satisfactory *in vivo* performance and flexibility in controlling the release of drugs with a broad range of physicochemical properties (1–3). Common hydrophilic polymers such as gelatin, hydroxypropylmethylcellulose, xanthan gum, hydroxpropylcellulose, polyethyleneoxide, polyvinyl alcohols, carbopol, and alginate that are employed in the formulation of monolithic matrices for controlled drug delivery have been extensively investigated (2–7).

Research has shown that drug release from hydrophilic monolithic matrices is mainly controlled by polymer erosion, disentanglement, dissolution and/or swelling front movement as well as drug dissolution and diffusion through the polymer matrix at the molecular level (2,3,8). These phenomena depend upon the interaction between the dissolution media, polymeric matrix and drug (3) and are influenced by several formulation variables, which include but are not limited to the drug concentration, drug solubility, polymer particle size (5,8–10), drug to polymer mass ratio, polymer viscosity, polymer molecular mass (3,4,10) and the addition of different types and levels of formulation excipients (1,11–15).

Polyamide 6,10 (PA 6,10) is a hydrophilic even-even configured, poly-condensed, synthetic aliphatic polyamide. Synthetic aliphatic polyamides have found applications in drug delivery applications as multiple-unit systems such as microcapsules (16,17), hollow fibers (18), gelospheres (19) and monolithic matrices (20,21). In addition, they have been known to possess pertinent physical properties such as thermal and abrasion resistance, chemical inertness, high physicomechanical strength, hydrophilicity, a high level of purity after production and controlled matrix dissolution (17,18,20–34) that makes the polyamides attractive for use in drug delivery. Generally, polyamides can be described as non-toxic and biocompatible, which stems from their extensive clinical use as both absorbable and non-absorbable surgical sutures (35–40).

The present study attempts to explore the effects of formulation variables and excipients on the drug release dynamics of a PA 6,10-based monolithic matrix employing a mathematical

[1] Department of Pharmacy and Pharmacology, Faculty of Health Sciences, University of the Witwatersrand, 7 York Road, Parktown 2193, Johannesburg, South Africa.
[2] To whom correspondence should be addressed. (e-mail: Viness.Pillay@wits.ac.za)

analytical approach. Monolithic matrices fabricated from synthesized PA 6,10 have been previously investigated, and their potential to function as matrices for rate-modulated drug release was established (20,21). Nevertheless, to the best of our knowledge, no scientific report relating the impact of formulation variables and excipients to the drug delivery characteristics of these unique delivery systems have been published. This is of particular importance since changes in formulation variables may further modulate the established drug release performance of the matrices and possibly broaden its drug delivery applicability. Therefore, this investigation focuses on establishing the influences of relevant formulation variables and excipients on the drug release performance from a PA 6,10 monolithic matrix. Amitriptyline hydrochloride (100% water soluble at 25°C) (41) and theophylline (0.85% water soluble at 25°C) (41) were respectively employed as model high and low solubility drugs in this study.

EXPERIMENTAL SECTION

Materials

Hexamethylenediamine (M_w=116.2 g/mol), sebacoyl chloride (M_w=239.1 g/mol), cyclohexane, anhydrous n-hexane, anhydrous sodium hydroxide pellets, amitriptyline HCl and theophylline were purchased from Sigma Chemical Company (St. Louis, USA). Poly (lactide-co-glycolide) (PLGA), resomer 202 was obtained from Boehringer Ingelheim (Ingelheim, Germany), hydroxypropylmethylcellulose (HPMC) K4M from Dow Chemical Company (Midland, Michigan, USA) and poly (ethylene oxide) (PEO) WSR-303 purchased from Union Carbide Corporation (Danbury, USA). Aluminium sulphate [$Al_2(SO_4)_3$] and magnesium sulphate ($MgSO_4$) were supplied by Merck Chemicals (Darmstadt, Germany), while potassium sulphate (K_2SO_4) was obtained from Rochelle Chemicals (Johannesburg, Gauteng, South Africa). All other reagents employed were of analytical grade and used as received.

Preparation of the PA 6,10-Based Monolithic Matrices

PA 6,10 was synthesized using modified interfacial polymerisation reaction previously described by Kolawole *et al.* (20). Each monolithic matrix comprised of a physical mixture of powdered PA 6,10 (300 mg) (particle size, 711–1,000 μm) and 50 mg of either of the model drugs with or without the respective formulation excipients throughout the study unless otherwise stated. Thorough mixing of the respective solids was carried out for about 15 min using a laboratory scale blender (CG 100, Kenwood Ltd., Cambridge, UK). Final blends were compressed into flat-surfaced, cylindrical monolithic matrices each having an average diameter of 13±1 mm and thickness of 4±1 mm using a Beckman hydraulic press (Beckman Instruments, Inc., Fullerton, USA) under a pressure of 1 ton, except stated, for 60 s.

Influence of Variations in Formulation Variables on the Drug Release Characteristics from the PA 6,10 Matrices

Selection of Model Drugs and Composition of Comparative Control Formulation

For the assessment of the impact of polymer–drug ratio, force of compaction, polymeric particle size and formulation excipients, amitryptiline hydrochloride was selected as the model drug because of its high water solubility, which makes it more suitable for determining the controlled release capability of the PA 6,10 monolithic matrix. However, theophylline and amitryptiline hydrochloride were employed as models for visualising the effects of drug solubility on the release characteristics of the PA 6,10 monolithic matrix. The control formulation (CF) for all the ensuing comparative experiments was made up of 300 mg PA 6,10 (particle size, 711–1,000 μm) and 50 mg of either model drug compressed at 1 ton.

Impacts of Variations in Drug Solubility, Polymer–Drug Ratio, Force of Compaction and Polymeric Particle Size

The impact of drug solubility on the release behaviour of the PA 6,10 monolithic matrix was assessed using 50 and 150 mg each of either amitryptiline hydrochloride or theophylline, respectively. The composition of each formulation employed to assess the effects of varying the polymer–drug mass ratio on drug release behaviour are presented in Table I. Different magnitudes of compaction forces ranging from 2.0, 3.0 and 4.0 tons were utilised for fabricating the matrices comprising 50 mg of amitryptiline hydrochloride and 300 mg PA 6,10. Textural analysis was used to determine the indentation hardness, which was computed as the Brinell hardness number (BHN). The BHN was used as a measure of matrix hardness or resistance to physicomechanical deformation due to an external compression force applied. A calibrated Texture Analyzer (TA.*XTplus*, Stable MicroSystems, Surrey, England) fitted with a ball probe of diameter 3.125 mm was employed for determining the peak force generated after indentation. The parameter settings employed were pre-test (2 mm/s), test (0.5 mm/s) and post-test (10 mm/s) speeds; trigger force (2 g); load-cell (5 kg); and indentation diameter of 1.563 mm. Data was captured at a rate of 200 points per

Table I. Composition of the Various Monolithic Matrices Utilised in Assessing the Effects of Polymer–Drug Ratio, Alternative Polymers and Electrolytes Using One-Variable-at-a-Time

	Composition			
Formulation	Amitryptiline (mg)	PA 6,10 (mg)	Alternative polymers (mg)	Electrolyte (mg)
1	50	200	–	–
2	50	100	–	–
3	50	50	–	–
4	50	450	–	–
5	50	600	–	–
6	100	300	–	–
7	200	300	–	–
8	300	300	–	–
9	25	300	–	–
10	50	300	PLGA: 300	
11	50	300	HPMC: 300	
12	50	300	PEO: 300	
13	50	300		K2SO4: 300
14	50	300		MgSO4: 300
15	50	300		Al2 (SO4)3: 300

second with Texture Exponent Software (Version 3.2). The BHN (N/mm^2) was calculated using Eq. 1.

$$BHN = \frac{2F}{\pi D\left(D - \sqrt{D^2 - d^2}\right)} \quad (1)$$

where F=force generated from indentation (N), D=diameter of ball probe indenter (3.125 mm) and d=indentation diameter (1.563 mm).

The impact of polymeric particle size was determined utilising laboratory test sieves (Endecotts Ltd, London, UK) with aperture sizes of 710 μm, 1.00 mm and 1.20 mm, which equates to particle size ranges of 1–710 μm, 711–1,000 μm (control) and 1,001–1,200 μm.

Effects of Alternative Polymers and Inorganic Excipients on the Release Dynamics of the PA 6,10 Monolithic Matrices

The influence of alternative polymers on drug release from the monolithic matrices was assessed using specific quantities of a mixture of PA 6,10 with PLGA or HPMC or PEO to prepare a monolithic matrix as stated in Table I.

The influence of inorganic electrolytes on drug release from the PA 6,10 monolithic matrices was explored utilising PA 6,10 blended with either K_2SO_4 or $MgSO_4$ or $Al_2(SO_4)_3$ (Table I).

Dissolution Studies

In vitro dissolution studies were performed on each set of monolithic matrix to investigate the influence of the abovementioned modulators on release kinetics. Each formulation was placed in a calibrated six-station dissolution testing apparatus (Caleva Dissolution Apparatus, model 7ST) using the standard USP 25 rotating paddle method at 50 rpm with 500 mL phosphate-buffered saline (PBS) (pH 7.4; 37±0.5°C). Five hundred milliliters PBS was used because no specific physiological condition was explored and also both model drugs, the electrolytes and alternative polymers as well as PA 6,10 dissolved sufficiently in it. The dissolution apparatus was modified by including a stainless steel ring mesh contrivance to prevent the hydrated formulation from floating (42). For the determination of the model drug concentration, 5 mL samples were withdrawn and filtered through a 0.45 μm pore size Cameo Acetate membrane filter (Millipore Co., Bedford, Massachusetts, USA) at specific time intervals over a period of 24 h. Samples were then analyzed by ultraviolet spectroscopy (Specord 40, Analytik Jena, AG) at 240 nm (amtryptiline hydrochloride) or 270 nm (theophylline). An equivalent volume to the quantity withdrawn of drug-free PBS was replaced into the dissolution medium to maintain sink conditions. A correction factor was appropriately applied in all cases where dilutions of samples were required, and all measurements were done in triplicate.

Treatment of Dissolution Data

With reference to the nature of this study, mathematical expressions were applied to facilitate thorough comparison and evaluation of the generated drug release data.

Model Independent Analyses

The explanation of the dissolution profiles using model independent methods encompassed the computation of specific dissolution quantities and fit factors discussed in the following sub-sections.

Time Point Approach

With this approach, $t_{x\%}$ (time required to release a specific amount of drug) values and mean dissolution times (MDT) set at $MDT_{x\%}$ (mean dissolution time of a specific amount of drug released) were computed. The application of t gives the specific time at which a certain amount of drug is released, while the MDT provides a more accurate view of the drug release behaviour as it is determined as the sum of the individual periods of time during which a specific fraction of the total drug dose is released (42–44). Equation 2 was employed in the calculation of the MDT.

$$MDT = \sum_{i=1}^{n} t_1 \frac{M_t}{M_\infty} \quad (2)$$

where M_t is the fraction of dose released in time t_i, t_i=(t_i+t_{i-1})/2, and M_∞ corresponds to the loading dose.

Fit Factors

Fit factors comprise of difference (f_1) and similarity components (f_2) (Eqs. 3 and 4) (1,42,45–48). These parameters compare and establish similarities and differences between two dissolution curves obtained from a set of experimental data (47). For this study, the f_2 component was utilised to evaluate selected drug release profiles (Eq. 3). When two profiles are similar, f_2 values range from 50 to 100 while f_2<50 indicate that the profiles are not similar (1,42).

$$f_2 = 50 \log\left\{\left(\left[1 + \frac{1}{n}\right]\sum_{t=1}^{n} w_t (R_t - T_t)^2\right)^{-0.5} \times 100\right\} \quad (3)$$

where R_t is the reference assay at time point t, T_t is the test assay at time point t, n is the number of pull points (or time points) and w_t is an optional weight factor.

Model Dependent Analysis

Kinetic Models

Usually, drug release from hydrophilic polymer based delivery systems have been described with the mechanisms of matrix relaxation and Fickian diffusion, which take place concurrently and are considered summative to the overall release performances (2,49). The well-known Peppas and Sahlin empirical model describes the abovementioned phenomenon. It is an expanded version of the power law, which

functions irrespective of the geometry of the drug delivery device (Eq. 4).

$$Q = \frac{M_t}{M_\infty} \quad = k_1\ t^m + k_2\ t^{2m} \tag{4}$$

where k_1 is the Fickian diffusion kinetic constant and k_2 is the relaxational or erosion rate constant, m is a kinetic constant and $Q = M_t/M_\infty$ is the fractional or percentage drug released in time, t (2,12,50,51). Generated dissolution data was fit into the Peppas and Sahlin model using Guassian–Newton approach for all least squares analyses on the WinNonlin Professional Edition, Version 5 (Pharsight, USA) and Sigma Plot, Version 11, (Systat Software Inc., California, USA).

Application of a Second-Order Polynomial Equation

The intrinsic values of fraction of drug released obtained at each time point was fitted into a second-order polynomial equation from which the fractional release rate constant (K_F in fraction/hour) was computed as the summative gradient for each profile. This parameter provided concise information as regards the drug release performances of the respective formulation under study and was useful for comparison of the dissolution profiles. All fitted curves were validated using the correlation coefficient, R^2 (values between 0.8 and 1 were considered relevant). In addition, the correlation factor (r), and p values were determined when necessary to assess the degree of relationship amongst data sets and level of linearity, respectively. The Sigma Plot, Version 11 software (Systat Software Inc., California, USA) was employed. Outcomes were presented as mean±standard deviation (SD).

Establishment of the Complexation Profile and Drug Release Mechanism via Static Lattice Atomistic Simulations

Computational modeling including energy minimisations in Molecular Mechanics was performed using HyperChem™ 8.0.8 Molecular Modeling Software (Hypercube Inc., Gainesville, Florida, USA) and ChemBio3D Ultra 11.0 (CambridgeSoft Corporation, Cambridge, UK). The three-dimensional (3D) structures of PA 6,10 (mPA), PLGA and PEO were archetyped using ChemBio3D Ultra in their syndiotactic stereochemistry, whereas the structure of HPMC (4 saccharide units) was built from standard bond lengths and angles using the Sugar Builder Module on HyperChem 8.0.8. The models were primarily energy-minimised using the MM+ force field algorithm and resulting structures subjected to energy minimisation using the Assisted Model Building and Energy Refinements 3 (AMBER 3) force field algorithm. The conformer having the lowest energy was used to develop the mPA-excipient and mPA-electrolyte complexes. A complex of one polymer molecule with another was assembled by parallel disposition and energy minimisation was repeated to generate the molecular complex models. Full geometrical optimisation was conducted in vacuum employing the Polak–Ribiere conjugate gradient method until a RMS gradient of 0.001 kcal/mol was reached (52). To generate the final models in solvated system, mPA-PLGA, mPA-HPMC, mPA-PEO, mPA-Al, mPA-K and mPA-Mg, simulations were performed for cubic periodic boxes with the polymer/polymer at the center of the cubic box and the remaining free space filled with water molecules. Energy minimisation was repeated to generate the solvated models except that the force fields were utilised with a distance-independent dielectric constant with no scaling (Table II). Additionally, the force field options in the AMBER (with explicit solvent) were extended to incorporate cutoffs to inner and outer options with the nearest-image periodic boundary conditions, which were applied to ensure that there were no discontinuities in the potential surface (Table II) (53).

RESULTS AND DISCUSSION

Impact of Formulation Variables on the Drug Release Characteristics of the PA 6,10 Monolithic Matrices

Solubility of Incorporated Model Drugs

Drug release profiles generated by the PA 6,10 monolithic matrices were comparable irrespective of the differences in solubilities of the loaded model drugs (r=0.998) at a 15% (50 mg) drug loading level ($f_2 \geq 50 \leq 100$) (Table III). An increase in drug loading to 35% (150 mg) showed a significant ($p<0.05$) difference (r=0.435) in the profiles in which case drug solubility had an influence on release rate ($f_2<50$). This was justified by determining the f_2 values at five dissolution time points ($t_{1\ h}$, $t_{6\ h}$, $t_{12\ h}$, $t_{18\ h}$ and $t_{24\ h}$) for each formulation (Table III). The dissolution profile generated for amitryptiline HCl was selected as reference while that of theophylline was the test and vice versa (Fig. 1).

Drug release from the PA 6,10 monolithic matrices at 15% drug loading can be said to be comparatively independent of drug solubility but mainly regulated by PA 6,10 matrix hydration or disentanglement. Nevertheless, the formulation containing amitryptiline HCl released slightly higher drug concentrations than that with theophylline at each time point (Table III). The influence of drug solubility on the release behaviour of the PA 6,10 matrix was more visible with an increase in drug loading to 35%. Overall, the release of amitryptiline HCl from PA 6,10 was faster than that of theophylline, and this pattern appeared to be more noticeable with an increase in drug concentration. This may be attributable to the higher hydrophilicity of amitryptiline HCl compared with theophylline (Fig. 1). Amitryptiline HCl enhanced outward influx of the dissolution medium resulting in the rapid dissolution and diffusion of drug molecules from the matrix, while theophylline possibly displayed an opposite behaviour

Table II. Typical Computational Parameters Used to Construct the Aqueous-Phase Model Building and Simulations for MPa with its Excipients/Electrolytes

Serial number	Parameters	Description
1	Periodic box dimensions	20×15×25 $A^{\circ 3}$
2	Cut-offs	Switched
3	Dielectric (epsilon)	Constant
4	1–4 scale factors	Electrostatic=0.5, van der Waals=0.5
5	Outer radius	7.5 A°
6	Inner radius	3.5 A°
7	Water molecules	236
8	Solvent/polymer distance	2.3 A°

Table III. Similarity Factors (F_2) for Assessing the Effects of Drug Solubility on Release Kinetics

Dissolution time points (h)	f_2 (15% amitryptiline loaded)	f_2 (35% amitryptiline loaded)
1.00	84.01	42.91
6.00	67.13	26.31
12.00	69.39	23.80
18.00	61.19	21.85
24.00	67.94	19.50

because of its lower solubility by increasing the matrix stiffness and hydrophobicity resulting in slower drug release kinetics.

Variation in Polymer Mass and Drug Ratios

The differences in the composition of the respective formulations had a considerable impact on the drug release dynamics and the discrepancies were further substantiated with the $MDT_{x\%}$ values. The $MDT_{10\%}$ and $MDT_{30\%}$ values were selected based on the fact that these dissolution points were common to all generated profiles (Fig. 2). An elevation or decline in the MDT values respectively indicated an increase or decrease in the duration required for a certain quantity of drug to be released.

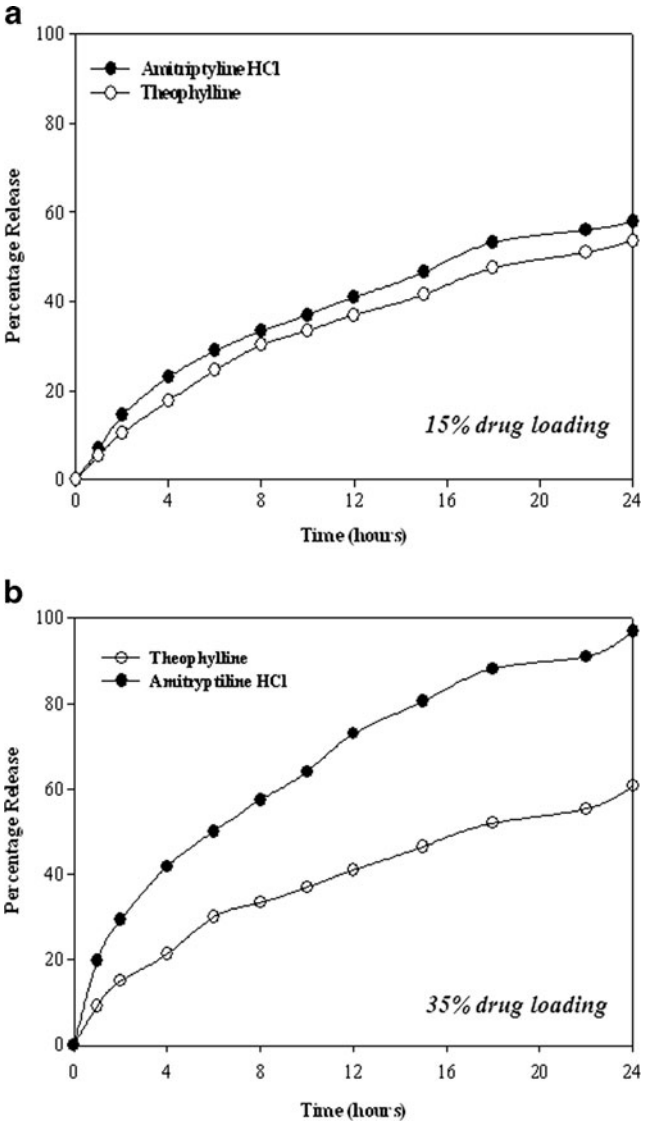

Fig. 1. The release profiles of amitryptiline HCl and theophylline loaded PA 6,10 matrix **a** 15% drug loading and **b** 35% drug loading (n=3 and SD ≤ 7.137% in all cases)

A decrease in polymer concentration as exemplified with formulations 1, 2 and 3, resulted in an increase in drug release substantiated with the computed $MDT_{10\%}$ (0.083, 0.051 and 0.029 h) and $MDT_{30\%}$ (1.383, 0.951 and 0.108 h), respectively when compared to the control ($MDT_{10\%}$=0.099 h; $MDT_{30\%}$= 1.570 h). An increase in burst levels, measured at $t_{1\ h}$ (12%, 20% and 35%, respectively) was observed with a decrease in PA 6,10 relative to the control ($t_{1\ h}$=7%). This can be attributed to the reduction in drug diffusion path length as a result of the reduction in polymer concentration. Consequently, the matrix is more susceptible to the impacts of hydration and disentanglement after the absorption of water molecules resulting in a quicker rate of drug diffusion. Formulations 4 and 5, containing a higher PA 6,10 concentration, displayed a decrease in drug release rates and burst levels ($MDT_{10\%}$=0.125 and 0.194 h; $MDT_{30\%}$=2.25 h and 3.245 h; $t_{1\ h}$=6%, 4%) when compared with the control ($MDT_{10\%}$=0.099 h; $MDT_{30\%}$=1.570 h; $t_{1\ h}$=7%). This may be as a result of an extension of the diffusion path length related to the increased polymer concentration. Furthermore, the trends observed for the release profiles of formulations 1–5 can be associated with their varying degrees of matrix permeability associated with the porosity levels of the respective matrices. In instances where polymeric concentration was reduced (formulations 1–3), the matrix upon hydration could be highly permeable with a low degree of tortuosity, minimal matrix strength, rapid erosion and quicker outward migration of drug molecules from the matrix while the reverse is the case when polymer concentration is higher (3). The PA 6,10 matrix demonstrated the potential to regulate drug release kinetics as formulation 3, which was composed of the lowest polymer concentration displayed the most rapid and irregular release pattern while formulation 5 with the highest polymer concentration showed the slowest, most consistent release characteristics (Fig. 2).

Profiles produced from formulations 6–9 displayed the effects of drug concentration on the PA 6,10 matrix. Generally, when compared to the control ($MDT_{10\%}$=0.099 h; $MDT_{30\%}$=1.570 h; $t_{1\ h}$=7%), an increase in drug concentration within the matrix amplified the release rates and burst-effects. Formulation 8 with the highest concentration of amitryptiline HCl elicited the most rapid drug release rate which was quantified by a lower $MDT_{10\%}$ and $MDT_{30\%}$ values (0.011 and 0.047 h, respectively). These outcomes were further substantiated by the elevated level of burst-effects of 47% determined at $t_{1\ h}$. On the contrary, formulation 9 contained the lowest amount of drug demonstrated a slower, more regulated release rate confirmed by the higher $MDT_{10\%}$ and $MDT_{30\%}$ (0.118 and 2.646 h, respectively) and a burst level at (6%). The observed pattern may be due to the ability of the hydrophilic amitryptiline HCl molecules to either increase or decrease the water uptake potential within the matrix as the drug loading levels increased or decreased respectively with the consequential effect of intensifying or minimising the velocities of matrix hydration, relaxation, dissolution and drug diffusion. Likewise, as drug loading increased (formulations 6–8), the release performance of the PA 6,10 matrices was by

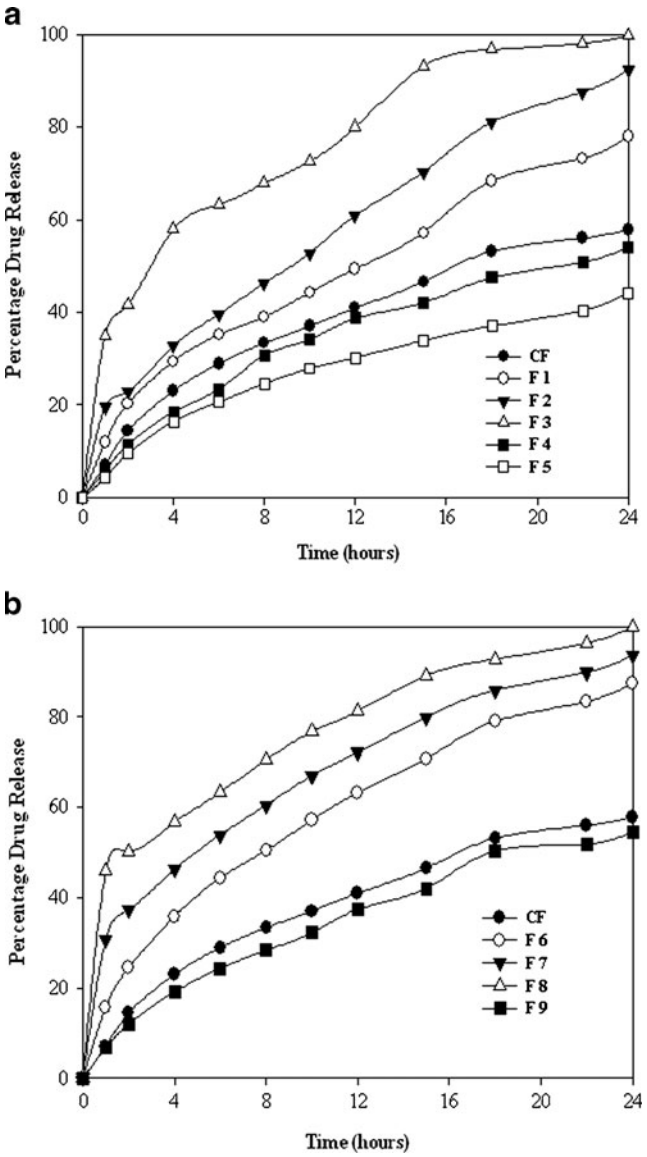

Fig. 2. Drug release profiles showing the effects of varying **a** polymer (PA 6,10) or **b** drug concentrations ($n=3$ and SD ≤ 10.015% in all cases)

matrix dissolution and drug diffusion. Thus, more water molecules were absorbed into the monolithic matrices, which probably enhanced the formation of continuous, intra-matrix interconnections that may have resulted in the formation of open pathways facilitating the outward diffusion of drug molecules while an opposite trend is expected at lower drug levels (formulation 9) (Table I, Fig. 2b).

Application of Different Forces of Compaction

Table IV outlines the changes in the magnitude of the measured mathematical quantities resulting from varying the applied force of compaction. A sequential increase in compression force from 1, 2, 3 and 4 t decreased the quantity of drug released over time. The observed changes in the drug release characteristics may be associated with an increase in the magnitude of inter- and intra-particulate electrostatic forces of attraction/cohesion amongst the polymer–polymer, drug–drug and/or polymer–drug particles as a result of the increase in the force of compaction. These proposed interactions can influence the packing capacity of the monolithic matrix resulting in an increased magnitude of the particulate cohesive interactions thereby enhancing matrix compactness and reduction in the rate of influx of water molecules into the matrix, thus retarding the rate of matrix wetting, extrication, dissolution, erosion and drug release. The $t_{x\%}$ values fixed at common dissolution points of $t_{10\%}$ and $t_{25\%}$ were employed to further corroborate the abovementioned propositions. An elevation in the force of compression from 1 (control) to 2–4 tons (as 4 tons was the maximum force that could be attained with the Beckman hydraulic press employed) of the had a significant ($p=0.0001$) elevating impact on the level of matrix hardness quantified by the BHN and $t_{x\%}$ values (Table IV). In other words, the differences in the BHN numerical values were vital measures for the degree of matrix firmness dependent on the magnitude of the forces of compression.

Influence of Polymeric Particle Sizes

The changes in PA 6,10 particle sizes considerably modulated release performance as an increase in particle size decreased the amount of drug released over time, while the reverse was the case for a decrease in particle size (Fig. 3). The reduction in particle size appeared to increase the surface area and wettability of the polymer and drug. Consequently, the water-absorbing capacity was impacted, thus making the hydrated more porous as a result of a reduced degree of tortuosity related to smaller particle size. However, with larger polymeric particle size, the extent of matrix wetting was reduced as the level of tortuosity may be higher leading to a minimised rate of disentanglement and diffusion of drug and a slower rate of drug release.

Table IV. Bhn and $T_{x\%}$ Values Demonstrating the Impacts of Changes Force of Compaction

		$t_{x\%}$ (h)	
Force of compression (tons)	BHN	$t_{10\%}$	$t_{25\%}$
1.00 (CF)	10.728±0.028	1.136±0.03	6.818±0.03
2.00	11.284±0.030	3.478±0.01	9.615±0.02
3.00	12.092±0.039	6.818±0.01	13.881±0.11
4.00	13.612±0.050	10.002±0.15	24.000±0.06

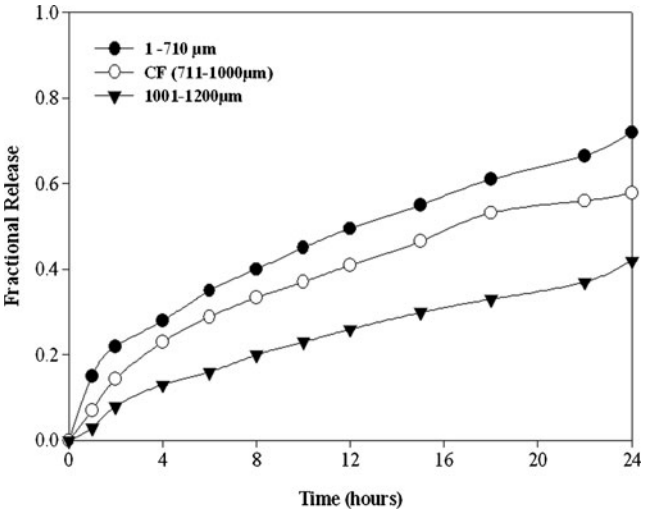

Fig. 3. Diverse impact of PA 6,10 particle size variation on the drug release behaviour from the PA 6,10 monolithic matrices (n=3 and standard deviation ≤ 0.08 in all cases)

Elucidating the Influence of Formulation Excipients on Drug Release Kinetics

Alternative Hydrophobic and Hydrophilic Polymeric Compounds

The inclusion of formulation excipients caused noteworthy disparities in exhibited drug release trends of the PA 6,10 matrix (Fig. 4). The most distinct release profile was that of formulation 10, which elicited a marked decrease in the amount of drug released over time when compared with the control formulation. This may be associated with the hydrophobic nature of PLGA, which implies that the hydrophilicity of PA 6,10 within the matrix was noticeably lessened. Generally, a slight but significant (p=0.035) dissimilarity was observed between the matrix containing HPMC and the control. However, HPMC, due to its hydrophilic nature, minimally enhanced the water-absorbing capacity of the matrix resulting in a slight elevation in the quantity of drug released (Fig. 4). In addition, this minimal impact of HPMC inclusion on release behaviour with reference to the control may be due to the capability of HPMC to undergo extensive dimensional swelling caused by an increase in viscosity during matrix wetting. This influenced the polymeric free volume and constituted a mechanism that HPMC employs to modulate drug release from the matrix (4,7,13,54,55). Furthermore, the matrix composed of PEO generated profiles showing increase in the amount of drug released over time. The hydrophilic nature of PEO as well as its minimal swelling tendencies, which can enhance and stabilise drug release velocities, respectively, could also have served as a contributing factor to the drug release behaviour.

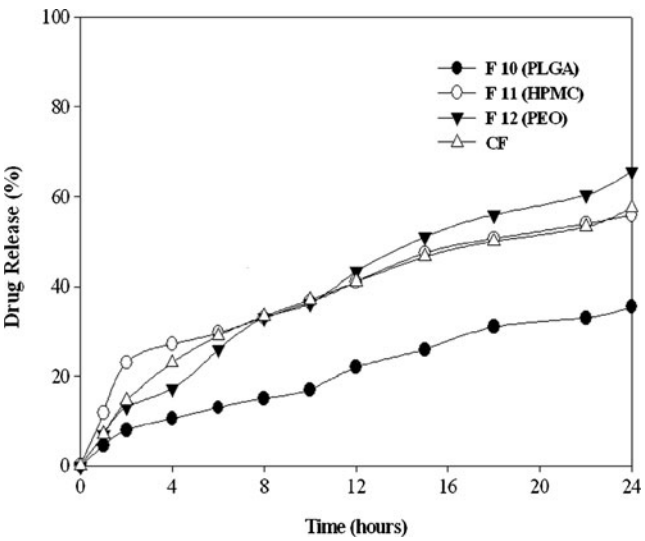

Fig. 4. Drug release profiles illustrating the effects of PLGA, HPMC and PEO on the drug release characteristics of the PA 6,10-based monolithic matrices (n=3 and SD ≤ 5.98% in all cases)

Besides the above-mentioned propositions, drug release profiles were separately fitted into the Peppas and Sahlin mathematical model to assess the contributions of the polymeric additives to the diffusional and relaxational phases of drug release from the PA 6,10 matrix by computing k_1 (% $h^{-0.43}$) and k_2 (% $h^{-0.86}$), respectively (2,7). For this investigation $Q \leq 65.55\%$ and t=24 h were employed for the respective formulations. In addition, m=0.43 was employed as it was the most appropriate for the geometry (aspect ratio) of monolithic matrix systems being investigated as previously established by Durig and Fassihi (Eq. 4) (2).

With reference to the total duration of drug release, the profiles can be considered linear (R^2>0.90 ≤ 1.00; formulations 10, 11, 12 and CF with values of 0.942, 0.902, 0.948 and 0.926, respectively). In comparison, k_1 (formulations 10=7.861% $h^{-0.43}$; 11=14.267% $h^{-0.43}$; 12=14.899% $h^{-0.43}$ and CF=13.740% $h^{-0.43}$) had higher numerical values than k_2 (formulation 10=2.446% $h^{-0.86}$; 11=4.298% $h^{-0.86}$; 12=4.620% $h^{-0.86}$ and CF=4.261% $h^{-0.86}$). Formulation 10 differed from the others in that both the diffusional and relaxational contributions to the process of drug release were reduced as was observed with the decline in values from 13.740% $h^{-0.43}$ and 4.261% $h^{-0.86}$ (CF) to 7.861% $h^{-0.43}$ and 2.446% $h^{-0.86}$, and this can still be associated with hydrophobic tendencies of PLGA. Conversely, the presence of HPMC and PEO increased the diffusional and relaxational release constants. The values generated for PEO were slightly higher (k_1=14.899% $h^{-0.43}$ and k_2=4.620% $h^{-0.86}$) than those of HPMC (k_1=14.267% $h^{-0.43}$ and k_2=4.298% $h^{-0.86}$) in comparison to the control (k_1=13.74% $h^{-0.43}$ and k_2=4.261% $h^{-0.86}$). Essentially, the polymeric excipients influenced the diffusional and relaxational components of the overall process of drug release over 24 h and therefore modulated the release kinetics of the drug molecules from the PA 6,10 matrix.

Impact of Ionisable Inorganic Electrolytes

The inclusion of inorganic electrolytes played distinctive roles in modulating the release of drug from the PA 6,10 matrix. A relationship between the drug release and the valency of the cationic and anionic components of the electrolyte was observed (Fig. 5). The inorganic electrolytes minimised the overall quantity of drug released over time compared with the control. This was further substantiated by the computed fractional release rate constant, K_F, values. Formulation 15, containing cations with the highest valency (Al^{3+}), had the slowest release rate (K_F=0.009 fraction released/h) while formulation 13 containing the electrolyte with the lowest cationic valency (K^+) showed a

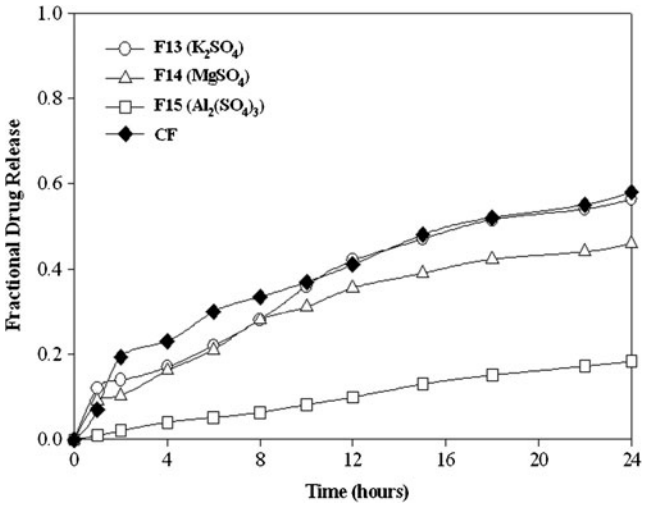

Fig. 5. Modulation of drug release from the PA 6,10-based monolithic matrix by inorganic electrolytes (n=3 and SD ≤8.37% in all cases)

quicker release rate (K_F=0.041 fraction released/h) in comparison with the control without electrolytes. Formulation 14 containing the divalent cationic electrolyte (Mg^{2+}) had a K_F value of 0.031 fraction released/h) in between those of (K^+) and (Al^{3+}). The observed trend can be related to the degree of hydration and hydrolysis of Al^{3+} in water because of its larger charge density and smaller orbital size compared with the water affinities of Mg^{2+} and K^+, which are much weaker because of their larger orbital sizes and smaller charge densities.

Furthermore, the pattern demonstrated by the electrolytes can be related to the phenomena proposed by Durig and Fassihi (2) as well as Pillay and Fassihi (13), which explained that a vital competitive interaction can exists between electrolyte and water species within a matrix system on exposure to the dissolution media during hydration. Consequently, the unionised electrolyte competes with the polymeric matrix for water species at the outset of influx. Therefore, the electrolyte, if more hydrophilic than the polymeric matrix attracts some of the water molecules within the matrix to dissociate into ionic components. This initial competition for water for hydration dehydrates the polymer matrix leading to suppression of initial polymeric wetting preceding drug diffusion. However, once sufficient water for hydrolysis has been attracted by the electrolyte within matrix microenvironment, the solubilised electrolyte species undergo an efflux process that possesses the potential to create porous channels within the hydrated matrix for the penetration of more water molecules, which then enhances polymeric matrix hydration, progressive matrix relaxation and outward drug diffusion.

With reference to the drug release characteristics demonstrated by the electrolytes included in the PA 6,10 matrix and the above-described phenomenon, it can therefore be proposed that the valency of the ions that constitute the test formulations influenced the interaction between the water molecules, polymeric components and respective electrolyte. This determined the extent of hydration based on the amount of water molecules required by each electrolyte for complete matrix hydrolysis into their ionic moieties. Furthermore, a competition between PA 6,10 and the respective electrolytes for water molecules may have occurred within the monolithic matrix. Based on the semicrystalline nature of PA 6,10 (28), the affinity of the electrolytes for water can outweigh that of PA 6,10 since the electrolytes are more crystalline and hydrophilic in nature. Therefore, the electrolytes set the pace with regards to the velocity of water infiltration into the respective matrices, and this subsequently influenced the rate of hydration of the polymeric matrix and ultimately the drug release efficiencies.

Hypothetically, it can be proposed that the higher the values of the cationic charges/charge densities (Al^{3+}), the greater the quantity of water molecules required to bring about a complete hydration and ionisation of the respective electrolyte species. This implied that there can be more competition for water molecules between the electrolyte and the polymeric component. Consequently, a higher level of polymeric dehydration is expected for matrices containing electrolyte species of this sort. This results in the suppression of drug release, as the process of polymeric matrix wetting which leads to breaking up of polymer chains leading to drug release was initially deactivated. At the point when sufficient water had been attracted by the electrolyte species for complete hydration and ionisation, then the ionised species can migrate out of the matrix creating considerable fissures within the matrix for water penetration, which can enhance matrix hydration, unfolding and drug release. For matrices containing cations with lower valences (K^+ and Mg^{2+}), the intensity of competition with the

Table V. Inherent Energy Attributes Representing the Molecular Assemblies Modelled Using Static Lattice Atomistic Simulations in the Solvated Phase

Molecular complex	$V_{\sum}$[a]	V_b[b]	V_θ[c]	V_φ[d]	V_{ij}[e]	V_{hb}[f]	V_{el}[g]
mPA-PLGA	−2316.51	24.54	44.03	35.89	5.27	−6.43	−2419.82
mPA-HPMC	−2895.04	29.56	85.96	11.42	49.55	−5.62	−3065.91
mPA-PEO	−3091.55	32.06	38.02	18.33	37.11	−2.23	−3214.84
mPA-Al	−2059.99	18.37	21.38	7.63	11.40	−3.13	−2115.64
mPA-Mg	−1982.99	18.19	21.27	7.59	37.46	0.00	−2067.50
mPA-K	−1951.76	19.19	85.01	8.42	1.67	0.00	−2066.05

[a] Total steric energy for an optimised structure
[b] Bond stretching contributions
[c] Bond angle contributions
[d] Torsional contribution associated with deviations from optimum dihedral angles
[e] van der Waals interactions
[f] Hydrogen-bond energy function
[g] Electrostatic energy

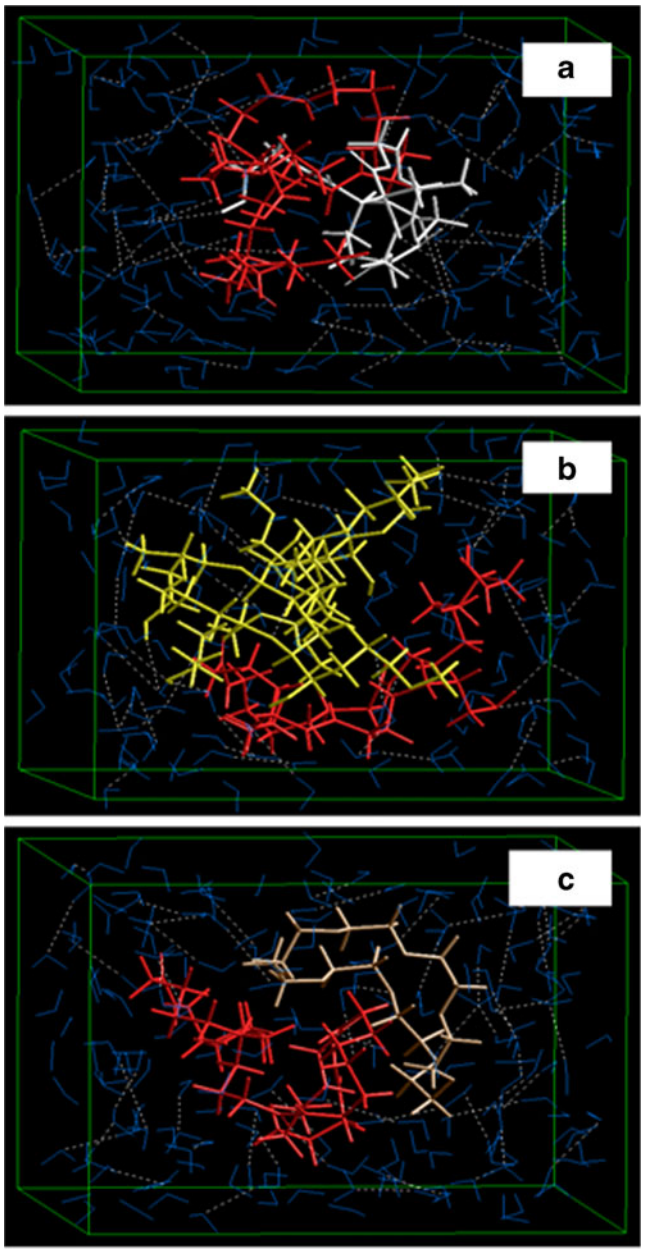

Fig. 6. Visualisation of geometrical preferences of **a** mPA-PLGA, **b** mPA-HPMC and **c** mPA-PEO after molecular simulation in a solvated system consisting of water molecules (*blue lines*). The mPA (*red*), PLGA (*white*), HPMC (*yellow*) and PEO (*brown*) are rendered in tube display

polymer for water molecules was milder because the amount of water required for complete hydration and ionisation was less. Therefore, the polymeric matrix was less dehydrated, and some level of hydration, disentangling and diffusion was initiated before the completely hydrated electrolyte species began to migrate out of the matrix to create more channels for water penetration that further enhanced drug release.

Overall, aluminium sulphate [$Al_2(SO_4)_3$] demonstrated the slowest release rate, while potassium sulphate (K_2SO_4) was the quickest and magnesium sulphate ($MgSO_4$) was in between these two extremes (*i.e.* $K^+ > Mg^{2+} > Al^{3+}$).

Outputs of Computational Modeling of the Excipient and Electrolyte Modified PA 6,10 Matrix

Effect of Polymeric Excipients

The component energy values related to mPA-PLGA, mPA-HPMC and mPA-PEO are shown in Table V, while the respective geometrically stabilised 3D conformations are displayed in Fig. 6. The mPA-PEO was most stabilised among the three mPA-excipient complexes with a total steric energy of ≈−3,092 kcal/mol as compared to ≈−2,895 kcal/mol and ≈−2316 kcal/mol for mPA-HPMC and mPA-PLGA, respectively (Table V). Interestingly, the stabilised energies for mPA-PEO

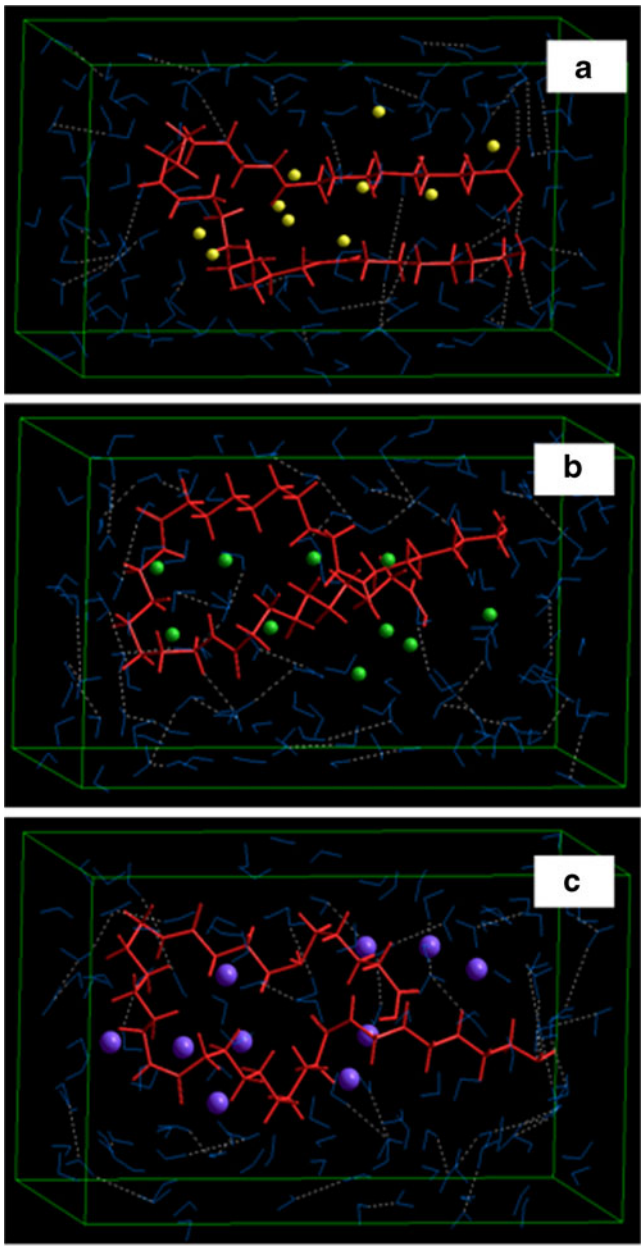

Fig. 7. Visualisation of geometrical representations of **a** mPA-Al, **b** mPA-Mg and **c** mPA-K after molecular simulation in a solvated system consisting of water molecules (*blue lines*). The mPA molecule (*red*) is rendered in tube display. Al (*yellow*), Mg (*green*) and K (*violet*) are rendered in ball displays

and mPA-HPMC were close in magnitude, and this relates very well with the similarity between their drug release profiles (Fig. 4). A faster drug release from mPA-PEO and mPA-HPMC may be attributed to the increased stabilisation of the complex in the vicinity of water molecules→increased affinity towards water→enhanced hydrophilicity of the matrix→increased access to the diffusion of water molecules into the matrix→higher drug release. An inverse relationship was observed for the mPA-PLGA formulation wherein the rate of drug release was reduced due to well-known hydrophobicity of PLGA. The polymer–excipient structures were mainly stabilised by the electrostatic interactions and hydrogen bonding component and were destabilised by all bonding energies (angle, bond and torsion energies) as well as the van der Waals forces. Conclusively, the non-bonding interactions balanced the torsional strain created by the bonding forces to accommodate the most feasible geometrical conformation as shown in Fig. 6.

Effect of Inorganic Electrolytes

The component energy values related to mPA-Al, mPA-K and mPA-Mg are shown in Table V, and the respective geometrically stabilised 3D conformations are displayed in Fig. 7. It is evident from Table V that mPA-Al was most stabilised among the three mPA-electrolyte complexes with a total steric energy of ≈−2,059 cal/mol as compared to ≈−1,982 kcal/mol and ≈−1951 kcal/mol for mPA-Mg and mPA-K, respectively. Interestingly, the stand-out stabilisation of mPA-Al supports the experimentally observed much slower drug release from F15 [$Al_2(SO_4)_3$] as compared to F13 (K_2SO_4) and F14 ($MgSO_4$) represented by mPA-K and mPA-Mg, respectively (Fig. 5). A slower drug release from more stabilised mPA-Al can be attributed to the increased stabilisation of the complex in the vicinity of water molecules→increased ionisation of the metal ion→increased cross-linking of the matrix structure→suppression of the initial polymeric wetting→slower drug release. The inverse is true for mPA-K and mPA-Mg formulations wherein the drug release rate was faster than mPA-Al due to a lesser amount of cross-linking prevailing in the monovalent and divalent cross-linked systems. Another reason for a slower drug release from mPA-Al may be attributed to hydrogen bonding (V_{hb}=−3.127; Table V) prevailing within the matrix leading to the formation of a well-knit polymer architecture, which was absent in the case of mPA-Mg and mPA-K molecular structures (Fig. 7). Similar to polymer–excipient complexes, the polymer–electrolyte structures were mainly stabilised by the electrostatic interactions and were destabilised by all bonding energies (bond, angle and torsion energies) as well as by the van der Waals forces.

CONCLUSIONS

In this study, the significant effects of formulation variables and excipients on the drug release performances of the novel PA 6,10-based monolithic matrix were investigated. The observed impacts revealed the robust and flexible, yet rate-modulated drug release behaviour and kinetics of the PA 6,10 matrix system, which resulted in the compilation of applicable deductions. Furthermore, the relevance of reputable mathematical expressions in assessing and comparing dissolution data as well as establishing the various possible drug release mechanisms of the PA 6,10 monolithic matrix was ascertained. The *in silico* lattice simulations for mPA-excipient and mPA-electrolyte complexes complemented the experimentally observed drug release profiles.

ACKNOWLEDGEMENTS

This work was funded by the National Research Foundation (NRF) of South Africa.

REFERENCES

1. Dürig T, Fassihi R. Evaluation of floating and sticking extended release delivery systems: an unconventional dissolution test. J Control Release. 2000;67:37–44.
2. Durig T, Fassihi R. Guar-based monolithic matrix systems: effect of ionizable and non-ionizable substances and excipients on gel dynamics and release kinetics. J Control Release. 2002;80:45–56.
3. Jamzad S, Tutunji L, Fassihi R. Analysis of macromolecular changes and drug release from hydrophilic matrix systems. Int J Pharm. 2005;292:75–85.
4. Shah N, Zhang G, Apelian V, Zeng F, Infeld MH, Malick AW. Prediction of drug release from hydroxylpropylmethylcellulose (HPMC) matrices: effect of polymer concentration. Pharm Res. 1993;10:1693–5.
5. Khurahashi H, Kami H, Sunada H. Influence of physicochemical properties on drug release rate from hydroxypropylmethylcellulose matrices. Chem Pharm Bull. 1996;44:829–32.
6. Yang L, Fassihi R. Modulation of diclofenac release from a totally soluble controlled release drug delivery system. J Control Release. 1997;44:135–40.
7. Reynolds TD, Gehrke SH, Hussain AS, Shenouda LS. Polymer erosion and drug release characterization of hydroxypropylmethylcellulose matrices. J Pharm Sci. 1998;87:1115–23.
8. Miyajima M, Koshika A, Okada J, Kusia A, Ikeda M. Factors influencing the diffusion-controlled release of papaverine from poly (L-lactic acid) matrix. J Control Release. 1998;56:85–94.
9. Yang L, Fassihi R. Examination of drug solubility, polymer types, hydrodynamics and loading dose on drug release behaviour from a triple-layer asymmetric configuration delivery system. Int J Pharm. 1997;155:219–29.
10. Velasco MV, Ford JL, Rowe P, Rajabi-Siahboomi AR. Influence of drug:hydroxypropylmethylcellulose ratio, drug and polymer particle size and compression force on the release of diclofenac sodium from HPMC tablets. J Control Release. 1999;57:75–85.
11. Pillay V, Fassihi R. Electrolyte-induced compositional heterogeneity: a novel approach to rate-controlled oral drug delivery. J Pharm Sci. 1999;88:1140–8.
12. Pillay V, Fassihi R. In situ electrolyte interactions in a disc-compressed system for up-curving and constant drug delivery. J Control Release. 2000;67:55–65.
13. Pillay V, Fassihi R. A novel approach for constant rate delivery of highly soluble bioactives from a simple monolithic system. J Control Release. 2000;67:67–78.
14. Williams III RO, Reynolds TD, Cabelka TD, Sykora MA, Mahaguna V. Investigation of excipients type and level on drug release from controlled release tablets containing HPMC. Pharm Dev Technol. 2002;7:181–93.
15. Hite M, Federici S, Turner S, Fassihi R. Novel design of a self-correcting monolithic controlled release system for tramadol. Drug Deliv Technol. 2005; Article Index: 1–13.
16. Torres D, Seijo B, García-Encina G, Alonso M, Vilajato JL. Microencapsulation of ion-exchange resins by interfacial nylon polymerization. Int J Pharm. 1990;59:9–17.
17. Chu L, Liang Y, Chen W, Ju X, Wang H. Preparation of glucose-sensitive microcapsules with a porous membrane and functional gates. Coll Surf B: Biointerf. 2004;37:9–14.

18. Ostad SN, Gard PR. Cytotoxicity and teratogenicity of chlorhexidine diacetate released from hollow nylon fibres. J Pharm Pharmacol. 2000;52:779–84.
19. Vyas SP, Sood A, Venugopalan P, Venkatesan N. Preparation and characterization of microencapsulated gelospheres for controlled oral theophylline delivery. J Microencap. 2000;17:767–75.
20. Kolawole OA, Pillay V, Choonara YE. Novel polyamide 6,10 variants synthesized by modified interfacial polymerization for application as a rate-modulated monolithic drug delivery system. J Bioact Compat Polym. 2007;22:281–313.
21. Kolawole OA, Pillay V, Choonara YE, Du Toit LC, Ndesendo VMK. The influence of polyamide 6,10 synthesis variables on the physicochemical characteristics and drug release kinetics from a monolithic tablet matrix. Pharm Dev Technol. 2010;15:592–412.
22. Makino K, Mack EJ, Okano T, Wan Kim S. A microcapsule self-regulating delivery system for insulin. J Control Release. 1990;12:235–9.
23. Kiely DE, Chen L, Lin TH. Hydroxylated nylons based on unprotected esterified D-glucaric acid by simple condensation reactions. J Amer Chem Soc. 1994;116:571–8.
24. Chattaraj SC, Swarbrick J, Kanfer I. A simple diffusion cell to monitor drug release from semi-solid dosage forms. Int J Pharm. 1995;120:119–24.
25. Jones NA, Atkins EDT, Hill MJ, Cooper SJ, Franco L. Chain-folded lamellar crystals of aliphatic polyamides. Investigation of nylons 4 8, 4 10, 4 12, 6 10, 6 12, 6 18, and 8 12. Polym. 1997;38:2689–99.
26. Gaymans RJ, Sikkema DJ. Aliphatic polyamides. In: Allen SG, Bevington CB, Price C, editors. Comprehensive polymer science. Oxford: Pergamon; 1999. pp. 357–73.
27. Murthy NS. Interactions between crystalline and amorphous domains in semi-crystalline polymers: small-angle X-ray scattering studies of the Brill transition in nylon 6,6. Macromol. 1999;32:5594.
28. Moniruzzaman M, Chattopadhyay J, Billups WE, Winey KI. Tuning the mechanical properties of SWNT/Nylon 6,10 composites with flexible spacers at the interface. Nano Lett. 2007;7:1178–85.
29. Li Y, Yan D, Zhu X. Crystal forms of nylon 10,12 crystallized from melt and after solution casting. Eur Polym J. 2001;37:1849–53.
30. Sikorsk P, Jones NA, Atkins EDT, Hills MJ. Measurement of the intersheet shear along the chain axis in nylon 6. Macromol. 2001;34:1673.
31. Ostad SN, Farhadkhani M, Minaiee B, Malihi G, Abdollahi M. The blood pressure and dermal sensitivity effects of nylon hollow fiber releasing glycerin trinitrate in vivo. Daru. 2002;10:125–9.
32. Fornes TD, Yoon PJ, Paul DR. Polymer matrix degradation and color formation in melt processed nylon6/clay nanocomposites. Polym. 2003;44:7545–56.
33. Cui X, Liu Z, Yan D. Synthesis and characterization of novel even-odd nylons based on undecanoic acid. Eur Poly J. 2004;40:1111–8.
34. Cui X, Yan D. Preparation, characterization and crystalline transitions of odd-even polyamides 11,12 and 11,10. Eur Polym J. 2005;41:863–70.
35. Van MW. The efficacy of a single continuous nylon suture for control of post keratoplasty astigmatism. Trans Am Ophthalmol Soc. 1996;94:1157–80.
36. Lundborg G, Dahlin L, Dohi D, Kanje M, Terada N. A new type of "bioartificial" nerve graft for bridging extended defects in nerves. J Han Surg (British and European Volume). 1997;22B:299–303.
37. Dolorico AMT, Ramin T, Hung VO, Ronald NG. Short-term and long-term visual and astigmatic results of an opposing 10–0 nylon double running suture technique for penetrating keratoplasty. J Americ Coll Surg. 2003;197:991–9.
38. Lee MJ, Patricia AD, Laurie AC. Aesthetic and predictable correction of the inverted nipple. Aesthet Surg J. 2003;23:353–6.
39. Seitz B, Langenbucher A, Küchle M, Naumann GOH. Impact of graft diameter on corneal power and the regularity of postkeratoplasty astigmatism before and after suture removal. Ophthalmol. 2003;110:2162–7.
40. Lai SY, Becker DG. Sutures and needles in Medscape: drugs, disease and procedure. 2004; pp. 1–13. http://www.emedicine.com/ent/topic38.htm. Accessed 26 Dec 2012.
41. Walter L. Principles and practice of pharmaceutics. In: Walter L, editor. The Pharmaceutical codex, 12th edn. London: The Pharmaceutical Press; 1994. pp. 1–1117.
42. Pillay V, Fassihi R. Evaluation and comparison of dissolution data derived from different modified release dosage forms: an alternative method. J Control Release. 1998;55:45–55.
43. Rinaki E, Dokoumetzidis A, Macheras P. The mean dissolution time depends on the dose/solubility ratio. Pharm Res. 2003;20:406–8.
44. Ansari M, Kazemipour M, Talebria J. The development and validation of a dissolution method for clomipramine solid dosage forms. Dissol Technol. 2004;17:20–4.
45. Moore JW, Flanner HH. Mathematical comparison of dissolution profiles. Pharm Tech. 1996;20:64–74.
46. Anderson NH, Bauer M, Boussac N, Khan-Malek R, Munden P, Sardaro M. An evaluation of fit factors and dissolution efficiency for the comparison of in vitro dissolution profiles. J Pharm Biomed Analys. 1998;17:811–22.
47. Sánchez-Lafuente C, Rabasco AM, Álvarez-Fuentes J, Fernández-Arévalo M. Eudragit® RS-PM and Ethocel® 100 Premium: influence over the behaviour of didanosine inert matrix system. Il Farmaco. 2002;57:649–56.
48. Costa FO, Sousa JJS, Pais AACC, Formosinho SJ. Comparison of dissolution profiles of ibuprofen pellets. J Control Release. 2003;89:199–212.
49. Pham AT, Lee PI. Probing the mechanisms of drug release from hydroxypropylmethylcellulose matrices. Pharm Res. 1994;11:1379–84.
50. Pillay V, Fassihi R. In vitro release modulation of cross-linked pellets for site-specific drug delivery to the gastrointestinal tract. I. Comparison of pH-responsive drug release and associated kinetics. J Control Release. 1999;59:229–42.
51. Siepmann J, Gopferich A. Mathematical modeling of bioerodible, polymeric drug delivery systems. Adv Drug Deliver Rev. 2001;48:229–47.
52. Kumar P, Choonara YE, Toit LC, Naidoo D, Pillay V. Novel high-viscosity polyacrylamidated chitosan for neural tissue engineering: fabrication of anisotropic neurodurable scaffold via molecular disposition of persulfate-mediated polymer slicing and complexation. Int J Mol Sci. 2012;13:13966–84.
53. Choonara YE, Pillay V, Ndesendo VM, du Toit LC, Kumar P, Khan RA, *et al*. Polymeric emulsion and crosslink-mediated synthesis of super-stable nanoparticles as sustained-release anti-tuberculosis drug carriers. Colloids Surf B Biointerfaces. 2011;87:243–54.
54. Siepmann J, Peppas NA. Mathematical modeling of controlled drug delivery. Adv Drug Deliver Rev. 2001;48:137–8.
55. Siepmann J, Peppas NA. Modeling of drug release from delivery systems based on hydroxylpropyl methylcellulose (HPMC). Adv Drug Deliver Rev. 2001;48:139–57.